General Predictive Syntheses of Cubic, Hexagonal, and Lamellar Silica and Titania Mesostructured Thin Films§

Peter C. A. Alberius,† Karen L. Frindell,† Ryan C. Hayward,‡ Edward J. Kramer,‡ Galen D. Stucky,*,† and Bradley F. Chmelka*,‡

Department of Chemistry and Biochemistry and Department of Chemical Engineering, University of California, Santa Barbara, California 93106

Received August 7, 2001. Revised Manuscript Received March 15, 2002

Well-ordered mesostructured silica and titania films were prepared using poly(ethylene oxide)−poly(propylene oxide)−poly(ethylene oxide) triblock copolymer species (Pluronic P123) as the structure-directing agents. By varying the volume ratio between the copolymer and inorganic components of the precursor solution, silica and titania thin films with cubic, 2D hexagonal, and lamellar mesostructures were prepared. The regions over which the three phases were obtained correspond well with those of the water−block copolymer binary phase diagram when considered in terms of the volume fraction of copolymer incorporated. In particular, a cubic mesostructure with crystalline TiO_2 (anatase) in the walls, stable to 400 °C, was synthesized.

Introduction

Since the discovery of surfactant-organized silicas and silicates in the early 1990s,[1−3] there has been extensive research in the field, motivated by the promise of these materials as catalyst supports, optical materials, sensors, low-*k* dielectrics, membranes, and selective adsorbents.[4−6] In the original preparations, alkaline conditions and cationic surfactants were used to organize mesostructures with relatively thin walls (∼1 nm) and limited hydrothermal stabilities. Nonionic amphiphilic block copolymers and surfactants were subsequently used to direct the formation of mesostructures with larger pore sizes, thicker walls (3−6 nm), and superior hydrothermal stabilities.[7−12] Many of these syntheses relied on a cooperative assembly mechanism between the organic structure-directing agent and the inorganic precursor species that resulted in the precipitation of powders from relatively dilute bulk surfactant solutions.[7,10,13−16]

Recently, there has been interest in the development of mesostructured materials for applications as optical waveguides, sensors, and membranes and in photovoltaic cells.[17−20] For these applications, it is important to control the mesophase ordering and macroscopic morphology adopted by the system. In such cases, it is advantageous to use more concentrated reaction mixtures under conditions in which the amphiphilic species form lyotropic liquid crystalline (LLC) -like mesophases into which inorganic precursor species are selectively incorporated. This approach provides significantly more flexibility in processing, allowing for the preparation of mesostructured monoliths,[8,9,21−26] thin films,[27−30] and fibers,[31] in addition to powders.

§ Presented in part at the American Physical Society Meeting, March 2001, Seattle, WA, and the American Chemical Society Meeting, April 2001, San Diego, CA.

* To whom correspondence should be addressed.
† Department of Chemistry and Biochemistry.
‡ Department of Chemical Engineering.

(1) Beck, J. S.; Vartuli, J. C.; Roth, W. J.; Leonowicz, M. E.; Kresge, C. T.; Schmitt, K. D.; Chu, C. T. W.; Olson, D. H.; Sheppard, E. W.; McCullen, S. B.; Higgins, J. B.; Schlenker, J. L. *J. Am. Chem. Soc.* **1992**, *114*, 10834−10843.
(2) Kresge, C. T.; Leonowicz, M. E.; Roth, W. J.; Vartuli, J. C.; Beck, J. S. *Nature* **1992**, *359*, 710−712.
(3) Yanagisawa, T.; Shimizu, T.; Kuroda, K.; Kato, C. *Bull. Chem. Soc. Jpn.* **1990**, *63*, 988−992.
(4) Stein, A.; Melde, B. J.; Schroden, R. C. *Adv. Mater.* **2000**, *12*, 1403−1419.
(5) Ciesla, U.; Schüth, F. *Microporous Mesoporous Mater.* **1999**, *27*, 131−149.
(6) Ying, J. Y.; Mehnert, C. P.; Wong, M. S. *Angew. Chem., Int. Ed.* **1999**, *38*, 56−77.
(7) Bagshaw, S. A.; Prouzet, E.; Pinnavaia, T. J. *Science* **1995**, *269*, 1242−1244.
(8) Attard, G. S.; Glyde, J. C.; Göltner, C. G. *Nature* **1995**, *378*, 366−368.
(9) Templin, M.; Franck, A.; Du Chesne, A.; Leist, H.; Zhang, Y.; Ulrich, R.; Schadler, V.; Wiesner, U. *Science* **1997**, *278*, 1795−1798.
(10) Zhao, D.; Feng, J.; Huo, Q.; Melosh, N.; Frederickson, G. H.; Chmelka, B. F.; Stucky, G. D. *Science* **1998**, *279*, 548−552.
(11) Lu, Y.; Fan, H.; Stump, A.; Ward, T. L.; Rieker, T.; Brinker, C. J. *Nature* **1999**, *398*, 223−226.
(12) Göltner, C. G.; Henke, S.; Weissenberger, M. C.; Antonietti, M. *Angew. Chem., Int. Ed.* **1998**, *37*, 613−616.
(13) Yu, C.; Yu, Y.; Zhao, D. *Chem. Commun.* **2000**, 575−576.
(14) Kim, J. M.; Stucky, G. D. *Chem. Commun.* **2000**, 1159−1160.
(15) Tanev, P. T.; Pinnavaia, T. J. *Science* **1995**, *267*, 865−867.
(16) Huo, Q.; Margolese, D. I.; Ciesla, U.; Feng, P.; Gier, T. E.; Sieger, P.; Leon, R.; Petroff, P. M.; Schüth, F.; Stucky, G. D. *Nature* **1994**, *368*, 317−321.
(17) Huo, Q. S.; Zhao, D.; Feng, J. L.; Weston, K.; Buratto, S. K.; Stucky, G. D.; Schacht, S.; Schüth, F. *Adv. Mater.* **1997**, *9*, 974−978.
(18) Wirnsberger, G.; Scott, B. J.; Stucky, G. D. *Chem. Commun.* **2001**, 119−120.
(19) Tsai, C. Y.; Tam, S. Y.; Lu, Y.; Brinker, C. J. *J. Membr. Sci.* **2000**, *169*, 255−268.
(20) Grätzel, M. *Prog. Photovoltaics* **2000**, *8*, 171−185.
(21) Göltner, C. G.; Antonietti, M. *Adv. Mater.* **1997**, *9*, 431−436.
(22) Yang, P.; Zhao, D.; Margolese, D. I.; Chmelka, B. F.; Stucky, G. D. *Nature* **1998**, *396*, 152−155.
(23) Melosh, N. A.; Lipic, P.; Bates, F. S.; Wudl, F.; Stucky, G. D.; Fredrickson, G. H.; Chmelka, B. F. *Macromolecules* **1999**, *32*, 4332−4342. Melosh, N. A.; Davidson, P.; Chmelka, B. F. *J. Am. Chem. Soc.* **2000**, *122*, 823−829.
(24) Göltner, C. G.; Berton, B.; Kramer, E.; Antonietti, M. *Adv. Mater.* **1999**, *11*, 395−398.
(25) Feng, P.; Bu, X.; Stucky, G. D.; Pine, D. J. *J. Am. Chem. Soc.* **2000**, *122*, 994−995.
(26) Feng, P.; Bu, X.; Pine, D. J. *Langmuir* **2000**, *16*, 5304−5310.

10.1021/cm011209u CCC: $22.00
Published on Web 07/13/2002

Thermodynamically equilibrated silica−surfactant LLCs have been produced under highly basic conditions, in which case the mesophase adopted could be controlled by adjusting the temperature or composition.[32−34] Mesostructured silica materials have more often been produced under nonequilibrium conditions, including by the acid hydrolysis of silicon alkoxides in the presence of organic structure-directing agents. This yields silica−surfactant mesophases that subsequently solidify as the silica cross-links. A number of groups have used water−surfactant phase diagrams to guide their syntheses of mesostructured hybrids.[8,9,11,21,24,27,29,30,35,36] In particular, several papers have described systematic approaches to controlling phase behavior by varying the ratio of silica to organic species, guided by the binary water−surfactant phase diagrams for ionic surfactant-,[29,30] block-copolymer-,[9,24] and nonionic surfactant-directed[8,36] mesostructures.

The primary objective of the present investigation is to demonstrate that by using published binary water−copolymer phase diagrams for commercially available Pluronic poly(ethylene oxide)−poly(propylene oxide)−poly(ethylene oxide) (PEO−PPO−PEO) triblock copolymers,[37−41] it is possible to predict directly the final mesostructural ordering adopted by silica− and titania−block copolymer composite thin films. A quantitative comparison can be made between the phase behavior of the water−block copolymer system and the observed nonequilibrium mesostructures, based on the volume fraction of the block copolymer in the quasi-liquid crystalline intermediate that is formed after the solvent is evaporated. We consider that the hydrophilic inorganic species swell the poly(ethylene oxide) block of the polymer and, to a first approximation, act as an equivalent volume of water. It is important to note that the system is not truly at equilibrium, and thus, the thermodynamic phase data must be augmented by some additional considerations. In particular, we find that the extent of condensation of the inorganic species in the solution from which films are prepared is important, as has been observed previously.[30]

This approach might be suitable for making a wide range of different mesostructured oxide materials, provided that a hydrophilic sol−gel precursor can be prepared under conditions where the oxide does not rapidly cross-link or crystallize. Here, we establish the case first for silica, providing detailed characterizations of the mesostructures obtained. We then extend the approach to titania, an inorganic oxide that has been of considerable technological interest in recent years.[20,42,43] In both cases, the same triblock copolymer ($EO_{20}PO_{70}EO_{20}$, Pluronic P123) was used to template lamellar, 2D hexagonal, and cubic mesostructures. The volume fractions of block copolymer required to form each structure agree well with the corresponding composition ranges for the water−block copolymer phase diagram.[37]

Experimental Section

Mesostructured Silica Thin Films. General approaches for preparing mesostructured silica thin films and monoliths have been described previously.[8,27,28,44−46] In the current investigation, silicon alkoxide species were first prehydrolyzed in an acidic water−ethanol solution with a pH close to the isoelectric point of silica (pH ≈ 2) to allow for hydrolysis of the alkoxides in a one-phase system under conditions of slow condensation.[47] Specifically, 10.4 g of tetraethyl orthosilicate (TEOS, 98% Aldrich) were prehydrolyzed in a solution containing 5.4 g of dilute hydrochloric acid (pH 2) and 12 g of ethanol under vigorous stirring at room temperature. The molar ratio between water and silicon was kept at 6 in all experiments to promote hydrolysis of the alkoxide species. Following 20 min of stirring at 20 °C, this prehydrolyzed silica solution was mixed with a solution containing the poly(ethylene oxide)−poly(propylene oxide)−poly(ethylene oxide) block copolymer $EO_{20}PO_{70}EO_{20}$ (Pluronic P123, BASF) dissolved in 8 g of EtOH. The amount of block copolymer added was chosen to produce a mesostructured film with the desired phase morphology (see Table 2 for detailed synthesis conditions). The solutions were then aged for between 10 min and 12 h, after which films were prepared by dip-coating (at a speed of 1 mm/s) onto the substrate. This resulted in continuous, transparent films with thicknesses 200−600 nm, depending on the copolymer concentration of the solution. Films were subsequently maintained at temperatures ranging from 5 to 35 °C for 24 h to increase the extent of silica cross-linking. The substrates used were glass slides, aluminized 0.125-mm-thick polyimide films (Sheldahl), and epoxy resins (Eponate 12, Ted Pella). X-ray transparent polyimide films were used as supports for the 2D SAXS measurements, whereas epoxy substrates were employed for the preparation of cross-sectional TEM specimens. Films deposited on glass slides were subsequently calcined by heating at a rate of 1 °C/min to 400 °C and holding for 4 h to remove the block copolymer species and increase cross-linking of the inorganic framework.

Mesostructured Titania Thin Films. During hydrolysis of the titanium alkoxides, highly acidic conditions were required to prevent immediate precipitation of TiO_2. Specifically, 4.2 g of titanium(IV) tetraethoxide (TEOT, 95% Aldrich) were dissolved in 3.2 g of concentrated hydrochloric acid (12.1

(27) Lu, Y.; Ganguli, R.; Drewien, C. A.; Anderson, M. T.; Brinker, C. J.; Gong, W.; Guo, Y.; Soyez, H.; Dunn, B.; Huang, M. H.; Zink, J. I. *Nature* **1997**, *389*, 364−368.
(28) Zhao, D.; Yang, P. D.; Melosh, N.; Feng, Y. L.; Chmelka, B. F.; Stucky, G. *Adv. Mater.* **1998**, *10*, 1380−1385.
(29) Honma, I.; Zhou, H. S.; Kundu, D.; Endo, A. *Adv. Mater.* **2000**, *12*, 1529−1533.
(30) Klotz, M.; Ayral, A.; Guizard, C.; Cot, L. *J. Mater. Chem.* **2000**, *10*, 663−669.
(31) Yang, P.; Zhao, D.; Chmelka, B. F.; Stucky, G. D. *Chem. Mater.* **1998**, *10*, 2033−2036. Melosh, N. A.; Davidson, P.; Feng, P.; Pine, D. J.; Chmelka, B. F. *J. Am. Chem. Soc.* **2001**, *123*, 1240−1241.
(32) Firouzi, A.; Atef, F.; Oertli, A. G.; Stucky, G. D.; Chmelka, B. F. *J. Am. Chem. Soc.* **1997**, *119*, 3596−3610.
(33) Firouzi, A.; Schaefer, D. J.; Tolbert, S. H.; Stucky, G. D.; Chmelka, B. F. *J. Am. Chem. Soc.* **1997**, *119*, 9466−9477.
(34) Tolbert, S. H.; Firouzi, A.; Stucky, G. D.; Chmelka, B. F. *Science* **1997**, *278*, 264−268.
(35) Coleman, N. R. B.; Attard, G. S. *Microporous Mesoporous Mater.* **2001**, *44*, 73−80.
(36) Attard, G. S.; Edgar, M.; Göltner, C. G. *Acta Mater.* **1998**, *46*, 751−758.
(37) Holmqvist, P.; Alexandridis, P.; Lindman, B. *J. Phys. Chem. B* **1998**, *102*, 1149−1158.
(38) Alexandridis, P.; Zhou, D.; Khan, A. *Langmuir* **1996**, *12*, 2690−2700.
(39) Alexandridis, P.; Olsson, U.; Lindman, B. *Langmuir* **1998**, *14*, 2627−2638.
(40) Wanka, G.; Hoffmann, H.; Ulbricht, W. *Macromolecules* **1994**, *27*, 4145−4149.
(41) Zhang, K.; Khan, A. *Macromolecules* **1995**, *28*, 3807−3812.
(42) Wijnhoven, J.; Vos, W. L. *Science* **1998**, *281*, 802−804.
(43) Grätzel, M. *Curr. Opin. Colloid Interface Sci.* **1999**, *4*, 314−321.
(44) Tolbert, S.; Schaffer, T.; Feng, J.; Hansma, P.; Stucky, G. *Chem. Mater.* **1997**, *9*, 1962−1967.
(45) Yang, H.; Coombs, N.; Sokolov, I.; Ozin, G. A. *Nature* **1996**, *381*, 589−592.
(46) Yang, H.; Kuperman, A.; Coombs, N.; Mamiche Afara, S.; Ozin, G. A. *Nature* **1996**, *379*, 703−705.
(47) Brinker, C. J.; Scherer, G. W. *Sol−Gel Science: The Physics and Chemistry of Sol−Gel Processing*; Academic Press: New York, 1990.

M) at room temperature under vigorous stirring. The molar ratio of water to titanium was kept at 6 in all experiments. After 5 min, a solution of P123 dissolved in 12 g of ethanol was added. Table 3 contains the specific amounts of P123 used for each phase. The solutions were subsequently aged with stirring at room temperature for between 15 min and 3 h before the films were dip-coated onto glass slides or ITO-coated polyester films (Sheldahl). Polyester films were used as supports for the 2D SAXS measurements. The dip-coating speed was 1 mm/s, and the films were aged at temperatures between 8 and 35 °C. Films deposited on glass slides were subsequently calcined by heating at a rate of 1 °C/min to 400 °C or 10 °C/min to 250 °C (2D hexagonal) and holding for 4 h to remove the block copolymer species and increase cross-linking of the inorganic framework.

Characterization. The samples were characterized by transmission electron microscopy (TEM), in combination with small-angle X-ray scattering (SAXS). Films were produced over a range of systematically varied compositions to determine the regions of existence for each phase. For simplicity, the detailed characterizations discussed below are limited to one particular composition for each structure.

A JEOL 2010 electron microscope operating at 200 kV was used for the TEM investigations. Plan-view film specimens were prepared by removing the films from the substrate with a razor blade and suspending them in ethanol. This suspension was then dispersed on a holey carbon film supported by a copper grid. Cross-sectional film samples were prepared by first dip-coating films directly onto an epoxy resin substrate. The mesostructured silica films were next covered with a 10−20-nm gold−palladium layer as a marker to aid identification in the TEM images and then embedded in an epoxy resin mold. Cross-sectional slices, ∼100 nm in thickness, were obtained by cutting with a diamond knife using an ultramicrotome.

X-ray diffraction measurements were performed using a Scintag X2 (Cu Kα radiation) powder diffractometer to acquire one-dimensional, out-of-plane diffraction patterns. Grazing-incidence two-dimensional SAXS experiments were also performed. Cu Kα radiation (1.54 Å) was generated with a fine-focus (0.2 mm) Rigaku rotating-anode generator and detected by a Bruker HI-STAR multiwire area detector (11-cm-diameter active area). The incident angle between the beam and film plane was varied between 2 and 10°, and the sample-to-detector distance was 1930 mm.

Simultaneous thermogravimetric analyses (TGA) and differential thermal analyses (DTA) were performed on a Netzsch STA 409 unit. Measurements were taken with a heating rate of 10 °C/min from 25 to 1100 °C.

Results and Discussion

Calculation of Block Copolymer Volume Fraction. We find that the mesostructures of the composite films can be predicted simply by considering the volume fraction of block copolymer (Φ) in the nonvolatile components of the solution. Grosso et al.[48] have shown by in-situ XRD experiments that the final mesostructure in block-copolymer-templated silica sol−gel films does not form until the ethanol and excess water used for prehydrolysis are evaporated. These components are therefore neglected in calculations of the volume fraction of block copolymer in the mesostructured composite. Considering only the block copolymer and inorganic precursor species, Φ is thus defined as

$$\Phi = V_{pol}/(V_{pol} + V_{inorg}) \quad (1)$$

where V_{pol} is the volume of the block copolymer present and V_{inorg} is the volume of the nonvolatile components in the solution. The definition of V_{pol} is straightforward

$$V_{pol} = m_{pol}/\rho_{pol} \quad (2)$$

where m_{pol} and ρ_{pol} are the mass and density of copolymer, respectively. The calculation of V_{inorg} involves some ambiguity, because the precise nature of the sol−gel precursors present when the mesostructure is formed is not known. As an approximation, the sol−gel precursors are considered to be fully hydrolyzed, uncondensed metal hydroxides. However, because of their instabilities,[47] reliable densities for pure $Si(OH)_4$ and $Ti(OH)_4$ are not available and must be estimated. Our results suggest that a reasonable approximation is to take the volume of these species to be equal to that of the dense inorganic compounds plus the water that is released during condensation.[49] In the case of titania, the volume of hydrochloric acid is included in the calculation of V_{inorg}, because it is apparently complexed with the titania species and hence incorporated to a significant extent into the films. Thus, V_{inorg} is defined as

$$V_{inorg} = \frac{m_{M(OH)_4}}{\rho_{M(OH)_4}} + \frac{m_{HCl}}{\rho_{HCl}} \approx \frac{m_{MO_2}}{\rho_{MO_2}} + \frac{m_{H_2O}}{\rho_{H_2O}} + \frac{m_{HCl}}{\rho_{HCl}} \quad (3)$$

where M = Si, Ti. We find that eqs 1−3 allow us to predict the structure for a given composition by locating the point on the binary water−P123 block copolymer phase diagram corresponding to the same volume fraction of polymer, Φ.

Table 1. Ranges of P123 Volume Percent (Φ) over Which the Different Mesophases Have Been Observed in the P123−Water,[37] P123−Silica, and P123−Titania Systems

	Φ_{P123} (%)		
mesostructure	H_2O−P123	SiO_2−P123	TiO_2−P123
lamellar	67−85	63−75	61−75
hexagonal	38−52	40−55	38−55
cubic	29−32	30−36[a]	29−36[a]

[a] Values for the cubic phase in the two P123−inorganic systems are for aging temperatures of 15 °C.

Below, a description is provided of how highly ordered mesostructured silica and titania thin films can be prepared with lamellar, 2D hexagonal (*p*6*mm*), and cubic morphologies using the same block copolymer (P123). In each case, the composition regimes over which the different mesostructures result correspond closely to the ranges of copolymer volume fractions associated with these phases in the binary P123−water phase behavior determined by Holmvqvist et al.[37] As summarized in Table 1 for both the silica−P123 and titania−P123 hybrid systems, the three phases were found over very similar ranges of composition. These ranges compare closely with those observed in the P123−water phase diagram, for example, differing by only 1−2% for the 2D hexagonal structure. This suggests that the self-assembly of the block copolymer is mostly sensitive to

(48) Grosso, D.; Balkenende, A. R.; Albouy, P. A.; Ayral, A.; Amenitsch, H.; Babonneau, F. *Chem. Mater.* **2001**, *13*, 1848−1856.

(49) Using the densities of bulk silica glass (2.2 g/cm^3) and of water (1 g/cm^3), a density of 1.5 g/cm^3 was obtained for silicic acid. The mass of silicic acid was calculated from the amount of TEOS added to the solution. The density of $Ti(OH)_4$ was estimated from the density of amorphous TiO_2 (∼3 g/cm^3) and water, yielding 1.8 g/cm^3. In this case, HCl was also considered to be a nonvolatile component (complexed to Ti), and its density in the film is taken to be the same as that of HCl in water (1.7 g/cm^3).

the relative volume fractions of the hydrophilic and hydrophobic species, rather than to the precise nature of the species swelling the hydrophilic ethylene oxide component.

Lamellar SiO_2 Films. For the binary water−P123 block copolymer LLC system, the lamellar mesophase appears from 67 to 85 vol % block copolymer at 25 °C.[37] By comparison, lamellar SiO_2−block copolymer mesostructures were found between 63 and 75 vol % using eqs 1−3. Attempts to incorporate larger volume fractions of block copolymer led to macrophase separation, which produced cloudy or opaque films. The detailed characterizations discussed below were performed on films containing 70 vol % P123. The 1D X-ray diffraction data shown in Figure 1a indicate a *d* spacing of 100 Å for the as-synthesized film, which is somewhat smaller than the *d* spacing of 110 Å found in the lamellar phase of the water−P123 block copolymer system at slightly higher polymer content, ∼75 vol %.[37] The smaller *d* spacing of the silica mesostructure is probably due to a contraction of the silica framework as water evaporates and cross-linking and densification of the silica occurs. The lamellar mesostructure collapses upon calcination, as indicated by the nearly featureless XRD pattern for the calcined film in Figure 1a. 2D SAXS experiments show diffracted intensity exclusively out-of-the-film-plane (Figure 2a), indicating that the lamellar structure is well aligned with the lamellae parallel to the substrate. TEM images of as-synthesized silica−P123 thin film samples (400−500 nm thick) reveal only the step-like features observed in Figure 3a, where each gray scale likely corresponds to an integral number of lamellar planes stacked on top of each other.

Hexagonal SiO_2 Films. The 2D hexagonal (*p6mm*) mesostructure is found between 38 and 52 vol % block copolymer in the water−P123 system at room temperature.[37] For the silica−block copolymer hybrids, hexagonal mesostructures were found between 40 and 55 vol % block copolymer. Representative films prepared with 45 vol % polymer are characterized and discussed below. One-dimensional X-ray diffraction data, presented in Figure 1b, show only the (100) and (200) diffraction peaks and indicate a *d* spacing of $d(100) = 90$ Å out of the film plane. The absence of the (110) reflection, which is typically seen in the X-ray diffraction pattern for the hexagonal structure, is due to the orientation of the hexagonal unit cell with the *c* and *a* axes parallel to the film substrate. The *d* spacing obtained is somewhat smaller than the value of 120 Å reported for the hexagonal water−P123 mesostructure at the same copolymer content.[37] This relatively large difference is likely due to the anisotropic shrinkage normal to the film plane observed for this structure (see below). The *d* spacing of the hexagonal silica thin film decreased to 57 Å upon calcination at 400 °C (Figure 1b), although the reflections were retained, indicating preservation of the hexagonal mesostructural ordering.

The orientation of the 2D hexagonal structure was confirmed by 2D SAXS measurements in grazing incidence mode. In Figure 2b, the presence of intense (100) spots normal to the film plane and weaker (010) reflections indicate that the *a* axes are oriented parallel to the film plane, and the *c* axes are randomly oriented within the film plane, as illustrated schematically in Figure 2c. These findings are similar to those found for mesostructured silica films synthesized using cetyltrimethylammonium bromide (CTAB), as reported by Klotz et al.[50] It should be noted that the diffraction pattern in Figure 2b shows distorted hexagonal symmetry, which is due to the anisotropic shrinkage of the thin film geometry as the silica network cross-links and

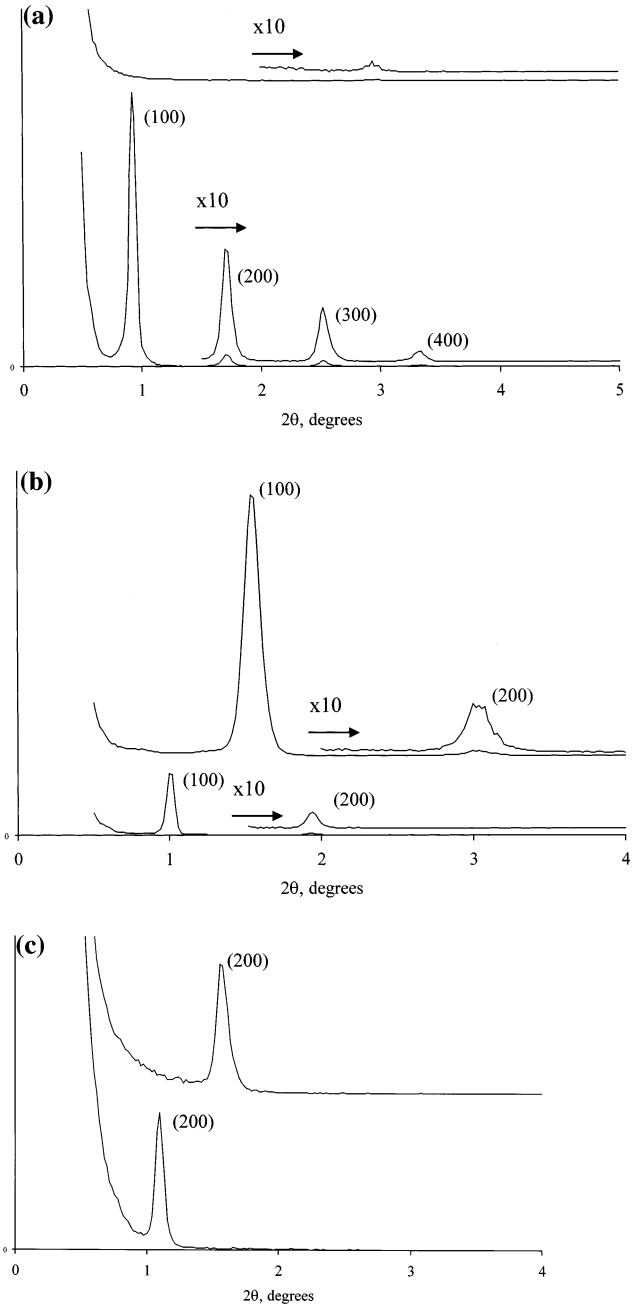

Figure 1. 1D X-ray diffraction patterns of different as-synthesized (bottom) and calcined (top) silica films approximately 200−500 nm in thickness with (a) lamellar, (b) hexagonal, and (c) cubic mesostructural ordering. The diffraction patterns are indexed according to the different symmetries (lamellar, 2D hexagonal *p6mm*, and body-centered-cubic $Im\bar{3}m$). The absence of, e.g., the (110) reflection in the hexagonal film is due to preferential orientational ordering of the cylindrical mesostructures parallel to the substrate.

(50) Klotz, M.; Albouy, P.-A.; Ayral, A.; Menager, C.; Grosso, D.; Lee, A. V. d.; Cabuil, V.; Babonneau, F.; Guizard, C. *Chem. Mater.* **2000**, *12*, 1721−1728.

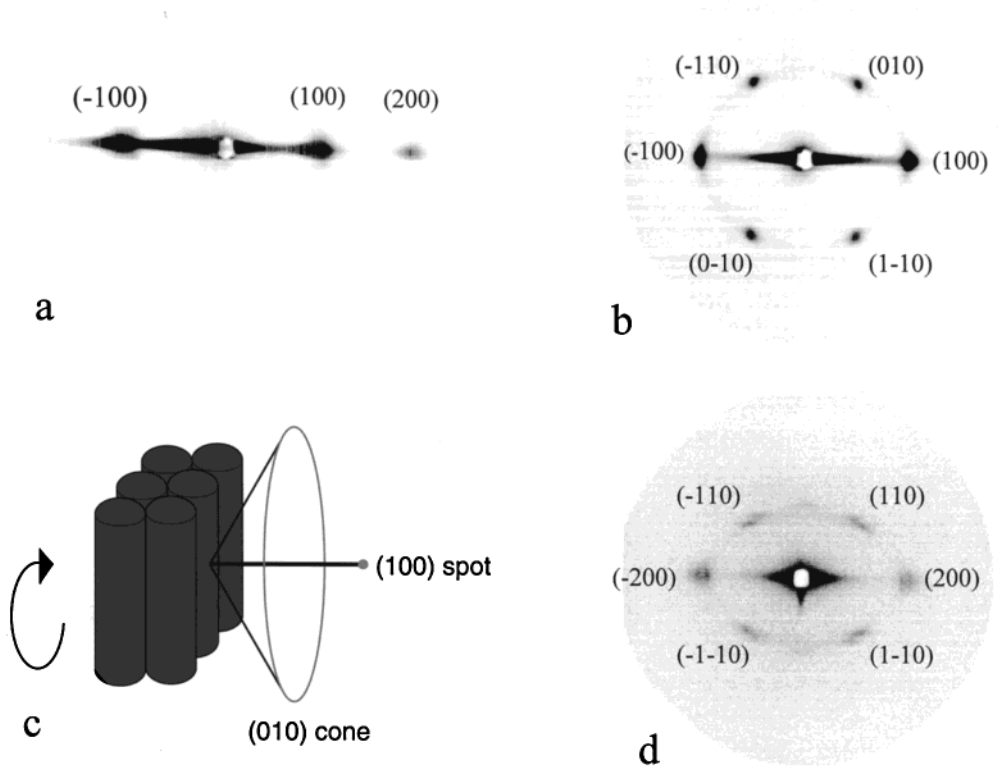

Figure 2. 2D SAXS diffraction patterns of as-synthesized (a) lamellar and (b) hexagonal mesostructured silica films. (c) Schematic drawing of the orientation of the hexagonal lattice and the corresponding pattern in reciprocal space. (d) Diffraction pattern from an as-synthesized cubic mesostructured silica film. The diffraction patterns are indexed according to the different symmetries for the three samples.

dries. Contraction occurs almost entirely normal to the film plane, resulting in a centered rectangular cell.[50] Measurements of *d* spacings from this diffraction pattern suggest that the hexagonal silica mesostructure has contracted by ~15% normal to the film plane.

Plan-view TEM images (Figure 3b,c) of the as-synthesized and calcined hexagonal mesostructured silica films show characteristic fingerprint-like patterns, which confirm that the cylinders are aligned parallel to the substrate but are randomly oriented within the plane. This morphology is consistent with structures observed previously in thin films of cylinder-forming block copolymers, where one of the polymer components preferentially wets the substrate or free interface.[51−53]

To study the domain sizes and uniformity of ordering within the films, cross sections of the as-synthesized films were prepared and examined by TEM. The resulting images reveal that the films are well-ordered throughout the film thickness (approximately 300−400 nm), with domain boundaries (marked by arrows in the TEM micrograph in Figure 3d) that extend perpendicular to the film plane. The average domain size observed was approximately 0.5 μm. In addition, the cross-sectioned samples provide further evidence of the orientational ordering of the hexagonal mesostructured domains. The TEM micrograph in Figure 3d shows regions with 2D hexagonal structure, in some of which the hydrophobic poly(propylene oxide) cylinders are directed out of the plane of the figure (left), whereas in others, the cylinders are oriented parallel to the image plane (right). In both cases, the *c* and *a* axes are oriented parallel to the substrate. Furthermore, the distortion of the hexagonal lattice due to shrinkage normal to the film plane can be measured directly from the image by measuring the lattice parameters parallel and perpendicular to the film plane. Specifically, the unit cell is contracted by 30% normal to the plane, giving rise to a 2D centered rectangular structure. This finding is in agreement with the work of Klotz et al.[50] on thin silica films, which examines the 2D hexagonal structure prepared using low-molecular-weight CTAB surfactant species. The distortion measured by TEM is about twice that determined from SAXS data, which might reflect compression of the silica film by the microtome blade during cross-sectioning of the sample.

It is interesting to compare the synthesis conditions of the hexagonally mesostructured silica films presented above with those of one of the few other examples of hexagonal mesostructures prepared using a liquid crystalline route and commercially available nonionic surfactants. Attard et al.[8] showed that, by using a 50 wt % surfactant ($C_{12}EO_8$ or $C_{16}EO_8$)−water mixture and adding 0.25 mol of tetramethyl orthosilicate (TMOS) per mole of water, a hexagonal silica mesostructure was formed (after removal of the methanol that was produced as the TMOS hydrolyzed). Using the formulas above, it is possible to estimate the fraction of surfactant

(51) Henkee, C. S.; Thomas, E. L.; Fetters, L. J. *J. Mater. Sci.* **1988**, *23*, 1685−1694.
(52) Coulon, G.; Russell, T. P.; Deline, V. R.; Green, P. F. *Macromolecules* **1989**, *22*, 2581−2589.
(53) Anastasiadis, S. H.; Russell, T. P.; Satija, S. K.; Majkrzak, C. F. *Phys. Rev. Lett.* **1989**, *62*, 1852−1855.

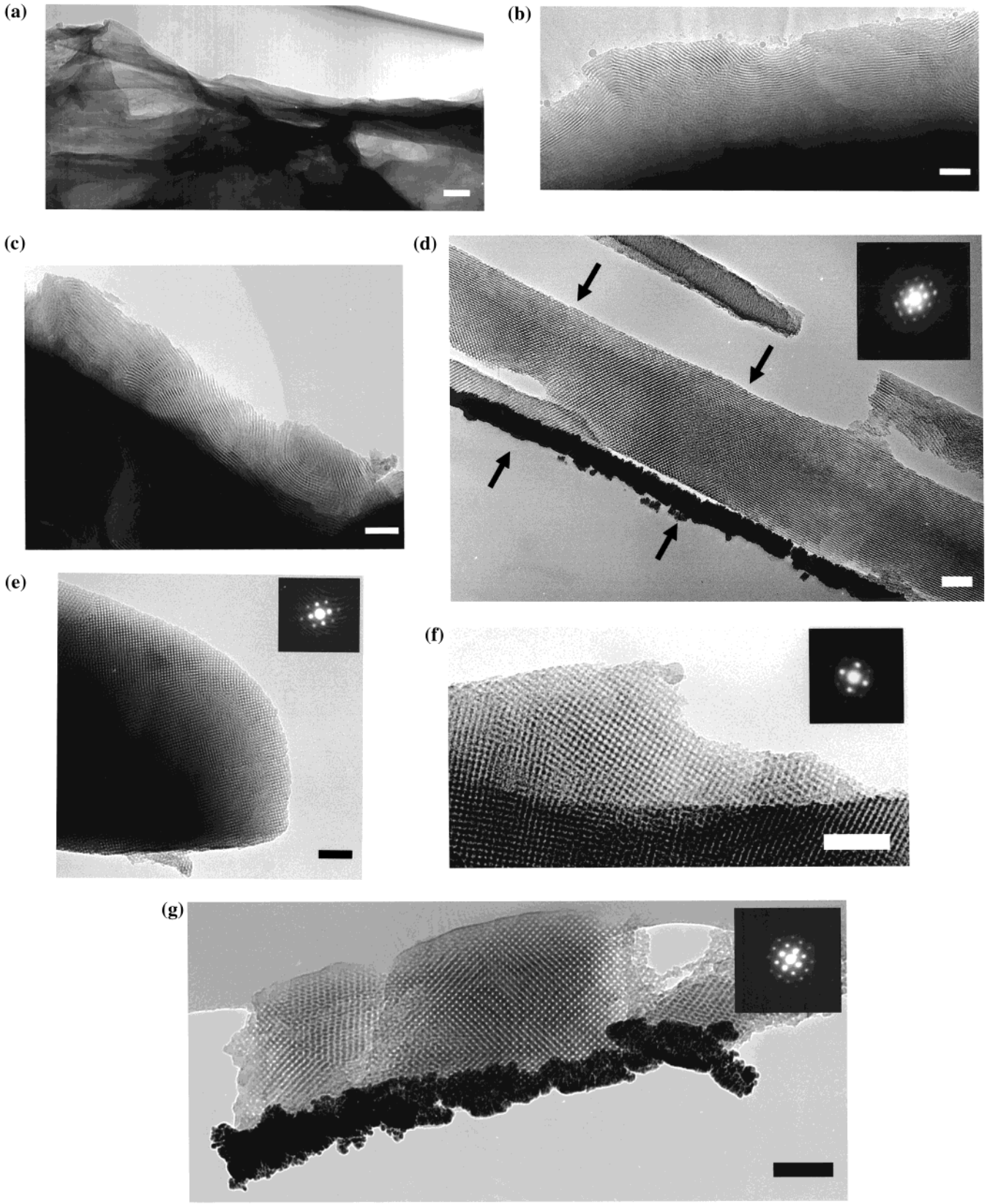

Figure 3. TEM micrographs of mesostructured silica films. Plan-view images of (a) as-synthesized lamellar, (b) as-synthesized hexagonal, and (c) calcined hexagonal films. (d) Cross-section of an as-synthesized hexagonal film showing that the *a* and *c* axes are parallel to the film plane. Plan-view images of (e) as-synthesized and (f) calcined cubic films and (g) a cross-section of an as-synthesized cubic film with {100} planes oriented parallel to the film. The insets in parts d−g are small-angle electron diffraction patterns from selected areas, recorded at an instrument camera length of 200 cm. The scale bars in the figures correspond to 100 nm.

in the silica−surfactant mesophase as 53 vol %, which corresponds to the hexagonal LLC region of the binary water−surfactant phase diagram.[54] They reported similar findings for water−surfactant mixtures in cubic and

lamellar lyotropic liquid crystalline phases.[8,36] The proximity in composition of the initial water−surfactant mixture to the final mesostructure is a result of the particular molar ratio of water to TMOS used. Instead of the weight fraction of surfactant in the initial surfactant−water mixture, it is more informative to estimate the volume fraction in the effective SiO_2−surfactant−water mixture that forms the mesostructure. This approach allows a quantitative prediction of the mesostructures formed, regardless of water content in the hydrolysis solution.

Cubic SiO_2 Films. The binary phase diagram of water−P123 at 25 °C has only a small concentration range over which the micellar cubic phase is stable (30−32 vol % block copolymer),[37] making it more challenging to produce cubic mesostructured silica films from P123 than hexagonal or lamellar films. In the present investigation, it was possible to form cubic mesostructured silica films at room temperature by incorporating 30 vol % block polymer, with the composition range extending to higher P123 content (36 vol %) for films aged at 15 °C. This result is consistent with the findings of Wanka et al.,[40] who showed that, in the binary water−P123 system at lower temperatures, the cubic phase occurs at higher block copolymer concentrations. Detailed characterization was performed on films prepared with 35 vol % P123 and aged at 15 °C. From the 1D X-ray diffraction pattern in Figure 1c, the *d* spacing of the as-synthesized cubic mesostructured silica film was found to be 81 Å, which diminished to 56 Å for the calcined film. The first peak in the diffraction pattern was indexed as the (200) reflection, because of the symmetry and orientation found in TEM images of these films (see below for discussion).

Plan-view TEM images show a well-ordered cubic mesostructure with micrometer-sized domains, as revealed in Figure 3e (as-synthesized) and 3f (calcined). These micrographs, together with cross-sectional TEM pictures (Figure 3g), suggest that the structure of the film is a micellar body-centered cubic ($Im\bar{3}m$) mesophase oriented with {100} lattice planes well-aligned parallel to the interface. If this is the case, these films should be similar to cubic mesoporous silicate SBA-16, whose structure was solved using TEM data.[55] The structure of SBA-16 closely follows the IWP minimal surface, which describes a body-centered-cubic micellar structure with open windows between neighboring micelles along the space diagonal of the cubic unit cell.[55] Indeed, the contrast in the electron micrographs shown in Figure 3e−g is the same as for images of SBA-16 recorded along the [100] crystallographic direction, indicating that the cubic silica mesophase seen here might also be $Im\bar{3}m$. In addition, some pieces imaged in plan view showed contrast corresponding to the [110] direction of the $Im\bar{3}m$ structure, suggesting the presence of mixed orientations within the film. As for the hexagonal films, the cubic mesostructure appears to be well-ordered throughout the film thickness (approximately 200−300 nm), with grain boundaries normal to the film plane (Figure 3g). Interestingly, the micrograph of the cross-sectioned sample appears to correspond to a nearly undistorted body-centered-cubic lattice viewed along the [010] zone axis. This suggests that the cubic mesostructure does not shrink normal to the film plane as extensively as the hexagonal mesostructure does.

The 2D SAXS diffraction pattern from a cubic mesostructured silica film is shown in Figure 2d. The diffraction spots are indexed as the (200) and (110) reflections, in accordance with the 1D diffraction data and the TEM investigations discussed above. Closer examination reveals two diffraction spots at each position denoted, as well as a weak reflection within the film plane. These extra spots provide further evidence that the film contains a mixture of domains with different orientations of the cubic unit cell relative to the film plane. The weaker spots are consistent with an $Im\bar{3}m$ body-centered-cubic (BCC) micellar structure with the {110} lattice planes oriented parallel to the film plane. The breadth and distribution of the diffraction peaks make it difficult to determine unambiguously the extent of shrinkage that has occurred normal to the film plane.

The orientation of the micellar body-centered-cubic mesophase in thin films has been previously investigated for the case of neat diblock copolymers. Yokoyama et al.[56,57] found that, in a poly(styrene-*b*-2-vinylpyridine) block copolymer that formed spherical domains, the presence of a silicon substrate induced layering with {110} lattice planes parallel to the film. These planes correspond to the most densely packed planes of the BCC unit cell. This orientational ordering is different from that observed in the cubic mesostructured silica films studied here, where predominantly the {100} planes were aligned parallel to the surface. The factors influencing orientational ordering of cubic mesostructures remain under investigation.

Effect of Aging Time on SiO_2 Films. Apart from the polymer-to-silica ratios and aging temperatures, there is an additional difference between the preparations of the lamellar, hexagonal, and cubic mesostructured thin films, namely, the optimal aging time of the solution before dip-coating. As shown by Klotz et al.,[30] to obtain well-ordered mesostructures, it is important that the siloxanes be sufficiently hydrolyzed before the films are processed, presumably because the presence of hydrophobic, nonhydrolyzed silicon alkoxides can disrupt ordering of the surfactant species. However, it is also crucial that the cross-linking of the silica not proceed too far. Klotz et al. found that, once Q^3 species appeared in solution, highly mesoscopically ordered silica−CTAB films could no longer be obtained.[30] Here, Q^n represents species with a central Si atom connected to *n* other Si atoms by Si−O−Si bonds ($n = 0-4$). If the silica species are extensively cross-linked, they begin to form a 3D network that cannot easily be formed into an ordered mesostructure by the organic structure-directing agents. Generally, as shown in Table 2, a substantially shorter aging time was required to produce cubic mesostructured films with well-defined long-range ordering, as compared to hexagonal and lamellar

(54) Mitchell, D. J.; Tiddy, G. J. T.; Waring, L.; Bostock, T.; McDonald, M. P. *J. Chem. Soc., Faraday Trans. I* **1983**, *79*, 975−1000.
(55) Sakamoto, Y.; Kaneda, M.; Terasaki, O.; Zhao, D. Y.; Kim, J. M.; Stucky, G.; Shin, H. J.; Ryoo, R. *Nature* **2000**, *408*, 449−453.
(56) Yokoyama, H.; Kramer, E. J.; Rafailovich, M. H.; Sokolov, J.; Schwarz, S. A. *Macromolecules* **1998**, *31*, 8826−8830.
(57) Yokoyama, H.; Mates, T. E.; Kramer, E. J. *Macromolecules* **2000**, *33*, 1888−1898.

Table 2. Synthesis Conditions for the Mesostructured SiO_2 Films[a]

mesostructure	Φ_{P123} (%)	P123 (g)	sol aging time (min)	aging T (°C)	d_{100} (Å)	d_{100}, calcined (Å)	calcination conditions
lamellar	70	7.70	180	10−35	100	−	−
hexagonal	45	2.75	180	10−35	90	57	400 °C, 4 h
cubic	35	1.70	10	5−15	81[b]	68[b]	400 °C, 4 h

[a] The amounts of H_2O (pH = 2 from HCl), TEOS, and ethanol were kept constant in each experiment at 5.4, 10.4, and 20 g, respectively. The ethanol was split into two portions, 12 g for the prehydrolysis solution and 8 g for the dissolution of the copolymer [b] The index of the first peak in the diffraction pattern of the cubic film is assigned to (200) based on the TEM and 2D SAXS characterizations.

films. The difference might arise from a lower stability of the cubic mesophase in the presence of large silicate oligomers, or could reflect the smaller region of composition space over which the cubic mesophase is found. This issue remains under investigation in our laboratories.

Mesostructured TiO_2 Thin Films. To illustrate the generality of the method described above for predicting the inorganic oxide−block copolymer mesostructures formed, the approach was extended to mesostructured titania films prepared with $EO_{20}PO_{70}EO_{20}$ (P123). Until recently, the only reported method for making thin films of well-ordered mesostructured TiO_2 was that of Yang et al.[22] Their procedure involved the alcoholysis of titanium tetrachloride by ethanol in the presence of amphiphilic block copolymers. Cross-linking of the inorganic network then occurred, through either a nonhydrolytic pathway or the slow hydrolysis of the titanium species by humidity in the surrounding atmosphere. Grosso and Soler-Illia et al.[58] recently modified this approach by adding additional water to the synthesis mixture and preparing films in a humid environment. They were able to use poly(ethylene oxide)-based structure-directing agents to prepare thin films of well-ordered 2D-hexagonal mesophase titania that were stable up to 350 °C.

In contrast to these previous reports, the current work applies the same approach to titania as in the silica preparations but uses a different pH in the prehydrolysis solution (pH ≈ −1). Such highly acidic conditions appear to stabilize titanium(IV) in solution[59] and were necessary to prevent immediate precipitation of TiO_2. When the mesostructured films are deposited, the inorganic species do not appear to cross-link irreversibly on a rapid time scale. The films remain soluble in ethanol for weeks after their preparation. To promote cross-linking, the titania films were heated to a minimum temperature of 130 °C. Apparently, the high concentration of chloride remaining in the film upon evaporation of ethanol and water stabilizes the titania species in the self-assembled mesophase, thereby slowing their condensation to form TiO_2 at room temperature. This stability of the titania intermediate species allows the block copolymer time to assemble into a stable nanophase-segregated structure and promotes formation of a mesoscopically well-ordered film. Although the presence of highly concentrated HCl has been observed to shift the LLC phase boundaries of the binary water−P123 system,[60] the titania−P123 mesophases formed under the very acidic conditions used here have ranges of stability with respect to both composition and temperature that are similar to those of the water−P123 and silica−P123 systems. This suggests that chloride is likely complexed with the titania species, such that the free HCl concentration in the mesostructured film is low.

Lamellar TiO_2 Films. To produce lamellar TiO_2 mesostructures, films were prepared with 63 vol % P123, as estimated from eqs 1−3. One-dimensional X-ray diffraction patterns acquired for the as-synthesized films (Figure 4a) show a d spacing of 110 Å. As for the lamellar silica films, the lamellar titania mesostructures collapse upon calcination. The 2D SAXS data, presented in Figure 5a, show only diffraction peaks out of the film plane, as expected from a well-aligned lamellar phase.

Hexagonal TiO_2 Films. Hexagonal TiO_2 mesostructures were produced using 55 vol % P123, as estimated from eqs 1−3. From the X-ray diffraction pattern in Figure 4b, the d(100) spacing was determined to be 107 Å. The mesostructure in the hexagonal titania films is stable up to a calcination temperature of 250 °C, with a temperature ramp rate of 10 °C/min. It is unclear why the hexagonal titania mesostructure, in particular, is not stable to calcination at higher temperatures. The 1D X-ray diffraction data in Figure 4b reflect a sizable contraction upon heating to 250 °C: d(100) decreased to 57 Å or by 47%. 2D SAXS measurements (Figure 5b) showed only very broad peaks normal to the film plane, indicating that the hexagonal TiO_2 mesostructured films are not as well-ordered as the equivalent SiO_2 films. Plan-view TEM micrographs of the calcined TiO_2 films (Figure 6a) show the same characteristic fingerprint pattern as of the hexagonal silica films, consistent with the 2D hexagonal mesophase morphology.

Cubic TiO_2 Films with Nanocrystalline Walls. Well-ordered cubic titania mesostructured films were prepared with a polymer content of 35 vol %, as estimated from eqs 1−3. As with the cubic silica mesostructures, the films were aged below room temperature, with the best results obtained at 8 °C. A d spacing of 90 Å was obtained from the 1D X-ray diffraction pattern of the as-synthesized titania film (Figure 4c), which was indexed in the same manner as the data for cubic mesostructured silica films, with the {100} planes of the unit cell oriented parallel to the substrate. Thus, the first peak observed in the diffraction pattern was indexed as the (200) reflection, assuming an $Im\bar{3}m$ space group (see below). The cubic films could be calcined at temperatures up to 400 °C without

(58) Grosso, D.; Soler-Illia, G. J. d. A. A.; Babonneau, F.; Sanchez, C.; Albouy, P.-A.; Brunet-Bruneau, A.; Balkenende, A. R. *Adv. Mater.* **2001**, *13*, 1085−1090. Soler-Illia, G. J. d. A. A.; Louis, A.; Sanchez, C. *Chem. Mater.* **2002**, *14*, 750−759.

(59) Baes, C. F.; Mesmer, R. E. *The Hydrolysis of Cations*; Wiley-Interscience: New York, 1976.

(60) Birefringence measurements on mixtures of 5 M hydrochloric acid with P123 indicated significantly different lyotropic liquid crystalline phase behavior than for equivalent samples prepared with deionized water.

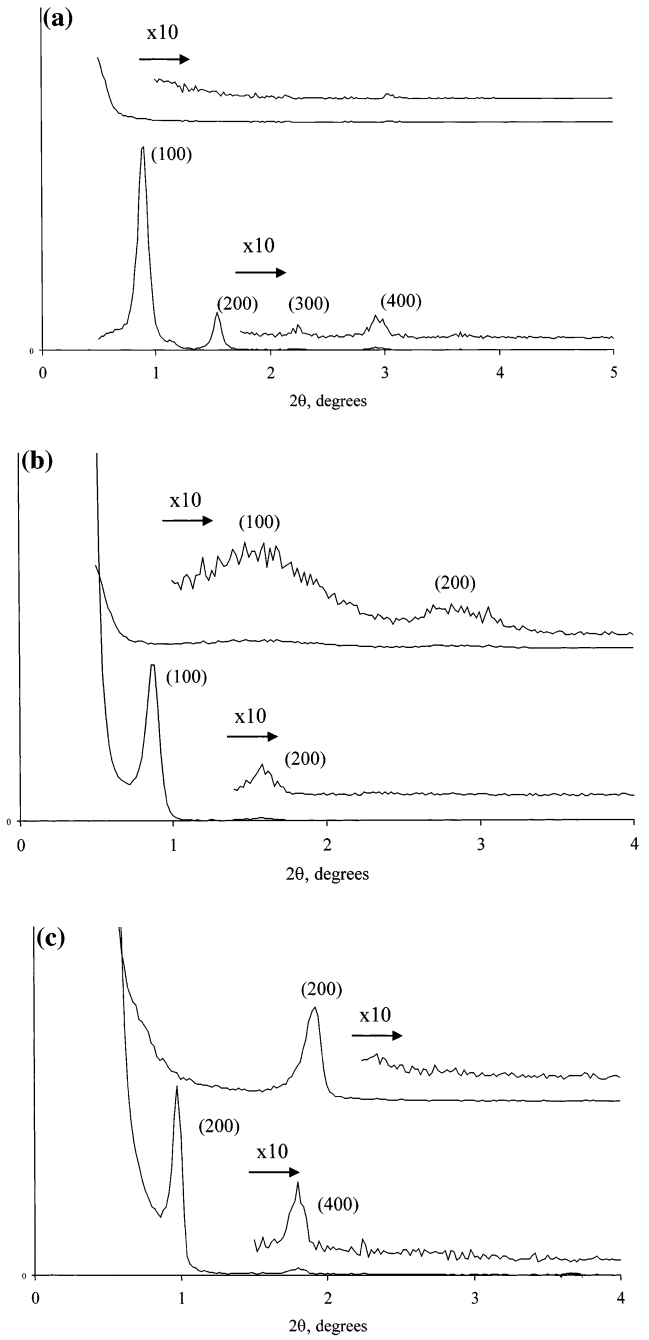

Figure 4. 1D X-ray diffraction patterns of mesostructured titania films approximately 200−500 nm in thickness. In each diffraction pattern, data are included from as-synthesized (bottom) and calcined (top) films for (a) lamellar, (b) hexagonal, and (c) cubic titania mesostructures. The diffraction patterns are indexed according to the different symmetries (lamellar, 2D hexagonal *p*6*mm*, and body-centered-cubic $Im\bar{3}m$).

loss of mesostructural ordering. The *d*(200) spacing decreased from 90 to 43 Å upon calcination. Judging from the TGA data discussed below, the large shrinkage was attributed to loss of HCl and densification of the TiO_2 walls. 2D SAXS measurements of the as-synthesized films (Figure 5c) show strong scattering reflections out of the film plane, indexed as (200) in accordance with the 1D diffraction data, confirming that the unit cells are relatively well-oriented with respect to the substrate. Broader reflections are also observed in the region where one would expect to see the (110) spots. Plan-view TEM micrographs recorded along the [100] zone axis, as shown in Figure 6b, display the same contrast as for the cubic mesostructured SiO_2 films and the corresponding images of SBA-16,[55] indicating that the cubic titania mesostructure might also have $Im\bar{3}m$ symmetry.

To investigate whether the walls of the calcined cubic mesoporous TiO_2 films contained crystalline regions, two different TEM methodologies were applied. It has previously been shown that dark-field images of mesostructured titania with semicrystalline walls show bright spots corresponding to nanocrystallites that scatter into an off-center objective aperture.[22] A similar experiment was conducted on the calcined cubic mesostructured TiO_2 film prepared here. As seen in Figure 6c, the micrograph clearly shows bright spots indicative of nanocrystalline TiO_2 particles scattering into the small-objective aperture used in the experiment. In addition, high-resolution TEM (HRTEM) images were recorded to resolve lattice fringes in crystallites within the walls of the cubic mesostructure. The micrograph in Figure 6d shows several randomly oriented nanocrystallites approximately 3−8 nm in diameter with clearly resolved lattice fringes, indicating that the walls are at least partially crystalline. Wide-angle X-ray diffraction patterns from this sample do not show any significant peaks, presumably because of the small sizes of the crystallites. However, we infer that the crystalline TiO_2 is anatase for three reasons. First, anatase is the crystalline form of TiO_2 typically formed at temperatures below approximately 600 °C.[61,62] Second, when the sample is calcined to 450 °C, the mesoscopic order is destroyed and peaks corresponding to anatase appear in the wide-angle X-ray diffraction patterns. The small "seed" crystallites observed in the sample calcined at 400 °C apparently grow in size at 450 °C, destroying the mesostructural ordering and producing grains large enough to be observed by X-ray diffraction. Finally, in Figure 6d, the enlarged crystallite has an interlayer *d* spacing of 3.5 Å, which corresponds well with the $d(101) = 3.52$ Å of anatase.[63]

To evaluate the temperature at which anatase begins to crystallize, thermogravimetric analysis (TGA) and differential thermal analysis (DTA) were performed on the as-synthesized cubic mesostructured TiO_2 film. The left curve in Figure 7 represents the DTA data, and the right curve the TGA results. Three features are seen in the DTA curve. At approximately 100 °C, a small endothermic peak is observed, which represents the removal of residual and adsorbed water, and at approximately 270 °C, an exothermic peak appears, corresponding to oxidation of the block copolymer species. The exothermic peak at approximately 460 °C most likely can be attributed to the amorphous−anatase transition of TiO_2. This is consistent with the TEM measurements that show evidence of semicrystalline walls in mesostructured TiO_2/P123 films calcined at 400 °C. The shift of the observed transition to higher temperature in the DTA experiment is likely a result of the rapid heating rate (10 °C/min), in contrast to the calcination where the sample is maintained at 400 °C

(61) Dachille, F.; Simons, P. Y.; Roy, R. *Am. Miner.* **1968**, *53*, 1931−1932.
(62) Ovenstone, J.; Yanagisawa, K. *Chem. Mater.* **1999**, *11*, 2770−2774.
(63) Cromer, P. T.; Herrington, K. *J. Am. Chem. Soc.* **1955**, *77*, 4708.

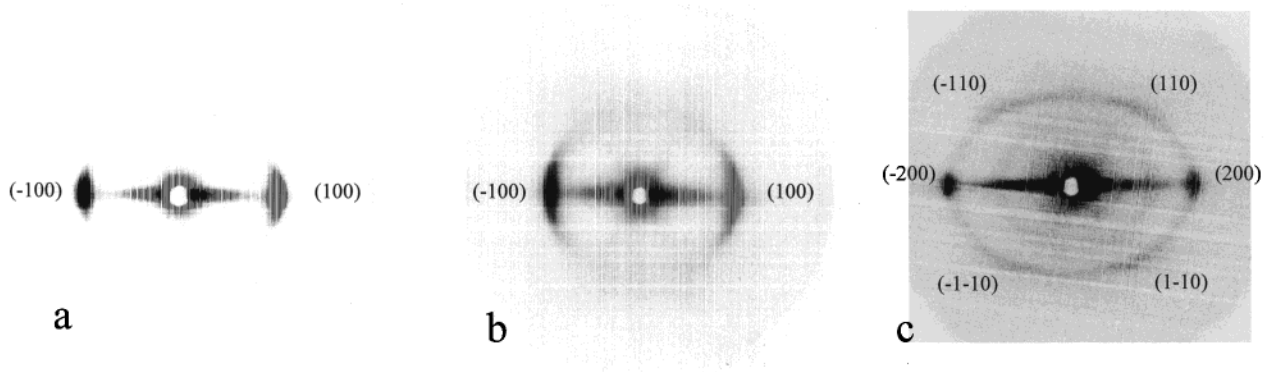

Figure 5. 2D SAXS diffraction patterns of as-synthesized mesostructured titania films: (a) lamellar, (b) hexagonal, and (c) cubic. The diffraction patterns are indexed according to the different symmetries for the three samples.

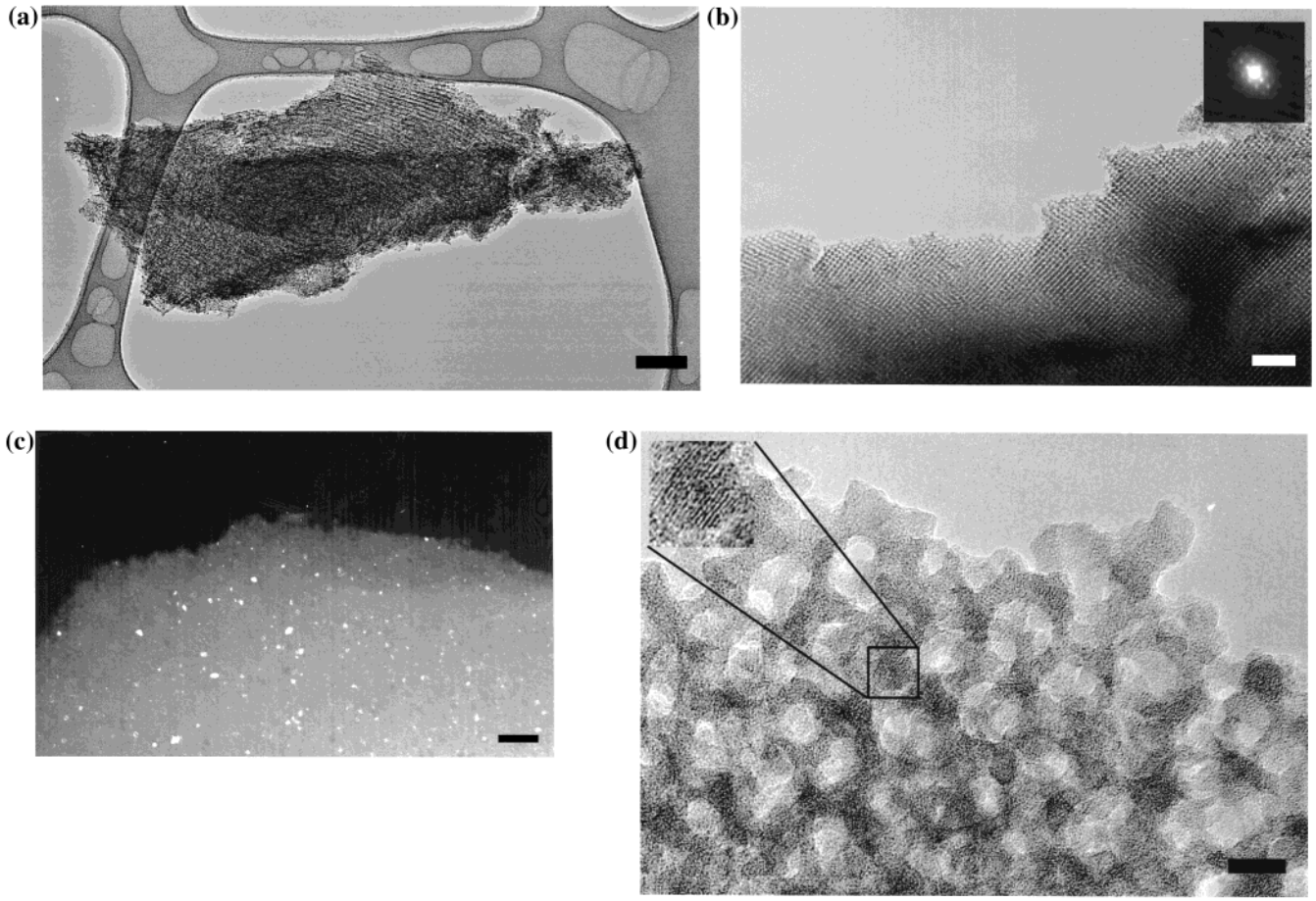

Figure 6. TEM micrographs of mesostructured titania films. (a) Plan-view image of a hexagonal film calcined at 250 °C. (b) Plan-view image of a cubic film calcined at 400 °C; the inset is a small-angle electron diffraction pattern from a selected area. (c) Dark-field TEM of a cubic film calcined at 400 °C; nanocrystallites diffract into an off-center objective aperture and thus appear bright. (d) A high-resolution micrograph of the cubic calcined film showing crystallites in random orientations with lattice fringes corresponding to the crystalline anatase structure. The scale bars in images a−c correspond to 100 nm and that in image d to 10 nm.

over a period of 4 h. In the region of 50−200 °C, the TGA curve shows a decrease in mass of ∼20%, which likely corresponds to the loss of water and HCl. The removal of the polymer block copolymer around 220−280 °C is accompanied by another decrease in the TGA curve of ∼20%.

Optimal aging times varied for the different structures. As for the mesostructured silica films, well-ordered cubic titania mesostructures were obtained after significantly shorter aging times than for the hexagonal and lamellar structures, as summarized in Table 3. The influence of solution aging on the degree of mesophase ordering remains under investigation.

Conclusions

We have presented a method for predictably controlling mesostructures of silica and titania in thin films, according to the binary water−$EO_{20}PO_{70}EO_{20}$ (P123) phase diagram. The relative concentrations of block copolymer and inorganic precursor species required to obtain a given mesostructure were estimated by ideal-

Table 3. Synthesis Conditions for the Mesostructured TiO_2 Films[a]

mesostructure	Φ_{P123} (%)	P123 (g)	sol aging time (min)	aging T (°C)	d_{100} (Å)	d_{100}, calcined (Å)	calcination conditions	TiO_2 framework
lamellar	63	3.12	180	10−25	110	−	−	−
hexagonal	55	2.30	180	10−25	107	57	250 °C, 4h	amorphous
cubic	35	1.00	10	8−15	90[b]	43[b]	400 °C, 4h	anatase

[a] The amounts of HCl (conc, 37% in H_2O), TEOT, and ethanol were kept constant in each experiment at 3.2, 4.2, and 12 g, respectively. [b] The index of the first peak in the diffraction pattern of the cubic film is assigned to (200) based on the TEM and 2D SAXS characterizations.

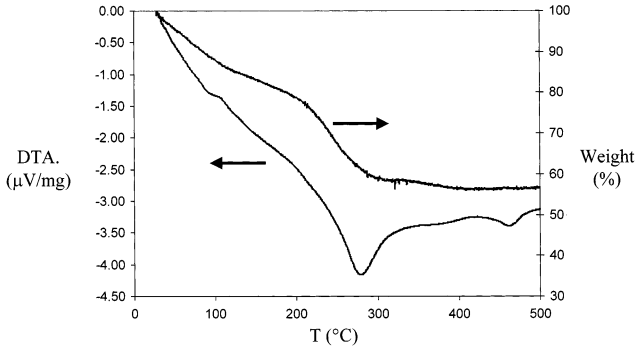

Figure 7. TGA (upper) and DTA (lower) data for a cubic mesostructured titania film. In the DTA trace, positive amplitudes correspond to endothermic reactions.

izing the multicomponent system as a two-component mixture and referring to the established water−polymer binary phase diagram in terms of the volume fraction of polymer incorporated. By employing inorganic precursor species that are hydrophilic but cross-link slowly, the self-assembling mixture can more closely approach a quasi-equilibrium structure dictated by the block copolymer and the relative amounts of hydrophobic and hydrophilic species.

This method should be general for directing the syntheses of co-assembling amphiphilic block copolymer−inorganic hybrid materials. Important criteria are that the inorganic precursor species must selectively swell one component of the block copolymer species and must cross-link on a time-scale that is slow compared to that of polymer self-organization. Furthermore, to idealize the system in terms of the binary water−polymer phase diagram, the inorganic components must not interact strongly with the organic structure-directing agent. There are a variety of amphiphilic block copolymers available whose binary polymer−solvent phase behaviors are well-known that display phases other than the ones shown here. By adjusting the molecular weight of the self-assembling block copolymer species, mesostructures can also be obtained with larger or smaller ordering length scales than displayed here. The generality of this method in terms of both organic and inorganic species suggests that it can be used to synthesize mesostructured metal oxide thin films with diverse compositions and structures.

There are a variety of interesting applications for mesostructured inorganic oxide films where control of the phase is important. For membranes and sensors, 3D connectivity is desirable to improve accessibility of pores and mass-transport properties. The hexagonal mesostructure might be useful in optical or electronic applications, because it presents a periodic array of channels with high aspect ratios that are, to some extent, isolated from one another. The lamellar films might prove to be useful in applications where regularly spaced sheetlike structures are desirable. Mesoporous semiconductors, such as anatase titania, have promise in the field of optoelectronic device fabrication. By intercalating dyes or other components into the mesostructure, these materials have potential to be used in solar cells, sensors, battery electrodes, and photocatalytic applications. In particular, the cubic TiO_2 mesostructure, which is stable to 400 °C and contains nanocrystalline anatase walls, might prove useful in photoelectronic and photocatalytic applications. Understanding the roles of the different components in establishing mesostructural ordering in inorganic−organic composite and inorganic mesoporous solids is important for optimizing these applications. General and predictive control of material composition and structure in these complicated heterogeneous nonequilibrium systems is improving.

Acknowledgment. This work was supported by the MRL Program of the National Science Foundation under Award DMR00-80034. P.A. acknowledges The Swedish Foundation for International Cooperation in Research and Higher Education and The Swedish Institute for funding. R.C.H. is a recipient of an NSF Graduate Research Fellowship.

CM011209U